Title
PET imaging of acetylcholinesterase inhibitor-induced effects on α4β2 nicotinic acetylcholine receptor binding

Journal
Synapse, 67(12)

ISSN
0887-4476

Authors
Hillmer, Ansel T
Wooten, Dustin W
Farhoud, Mohammed
et al.

Publication Date
2013-12-01

DOI
10.1002/syn.21698

Peer reviewed

Published in final edited form as:
Synapse. 2013 December ; 67(12): 882–886. doi:10.1002/syn.21698.

PET Imaging of Acetylcholinesterase Inhibitor Induced Effects on α4β2 Nicotinic Acetylcholine Receptor Binding

Ansel T Hillmer[1,2], **Dustin W Wooten**[1,2], **Mohammed Farhoud**[3], **Andrew T Higgins**[2], **Patrick Lao**[1,2], **Todd E Barnhart**[1], **Jogeshwar Mukherjee**[4], and **Bradley T Christian**[1,2,5]

Ansel T Hillmer: ahillmer@wisc.edu; Dustin W Wooten: dwooten@wisc.edu; Mohammed Farhoud: mfarhoud@wisc.edu; Andrew T Higgins: athiggins@wisc.edu; Patrick Lao: plao@wisc.edu; Todd E Barnhart: tebarnhart@wisc.edu; Jogeshwar Mukherjee: mukherjj@uci.ed; Bradley T Christian: bchristian@wisc.edu

[1]Department of Medical Physics, University of Wisconsin-Madison, Madison, WI 1111 Highland Ave, Room 1005, Madison, WI 53705

[2]Waisman Brain Imaging Laboratory, University of Wisconsin-Madison, Madison, WI 1500 Highland Ave, Madison, WI 53705

[3]Comprehensive Cancer Center, University of Wisconsin-Madison, Madison, WI 1111 Highland Ave, Room 7057, Madison, WI 53705

[4]Department of Radiological Sciences, University of California-Irvine, Irvine, California 101 The City Drive South, Route 140, Orange, CA 92868

[5]Department of Psychiatry, University of Wisconsin-Madison, Madison, WI 6001 Research Park Blvd, Madison, WI 53719

Abstract

Acetylcholinesterase inhibitors (AChEIs) are drugs that increase synaptic acetylcholine (ACh) concentrations and are under investigation as treatments for symptoms accompanying Alzheimer's disease. The goal of this work was to use PET imaging to evaluate alterations of *in vivo* α4β2 nicotinic acetylcholine receptor (nAChR) binding induced by the AChEIs physostigmine (PHY) and galanthamine (GAL). The α4β2 nAChR specific radioligand [^{18}F]nifene was used to examine the effects of 0.1–0.2 mg/kg PHY, 5 mg/kg GAL, and saline in three separate experiments all performed on each of two rat subjects. A 60 min bolus-infusion protocol was used with drug administered after 30 min. Data from the thalamus and cortex were analyzed with a graphical model accounting for neurotransmitter activation using the cerebellum as a reference region to test for transient competition with bound [^{18}F]nifene. Significant [^{18}F]nifene displacement was detected in both regions during one PHY and both GAL studies, while no significant competition was observed in both saline studies. This preliminary work indicates the viability of [^{18}F]nifene in detecting increases in synaptic ACh induced by AChEIs.

Keywords

PET; [^{18}F]Nifene; Nicotinic Acetylcholine Receptor; Acetylcholinesterase Inhibitors; Physostigmine; Galanthamine

Corresponding Author: Ansel T. Hillmer, M.S., Department of Medical Physics, University of Wisconsin-Madison, 1111 Highland Avenue, Madison, WI 53705, ahillmer@wisc.edu, Telephone: (608) 890-2959.

Introduction

Acetylcholine (ACh) is a neurotransmitter that modulates neurochemical transmission, and is involved in a wide variety of neuropsychiatric disorders (Hogg et al. 2003). In particular, the cholinergic hypothesis implicates a decline of the cholinergic system in the cognitive symptoms of Alzheimer's disease (Bartus et al. 1982). As a result, acetylcholinesterase inhibitors (AChEIs) have been used therapeutically to treat cognitive deficiencies accompanying Alzheimer's disease. AChEIs inhibit the hydrolysis of synaptic ACh to acetic acid and choline, thereby increasing synaptic ACh concentrations. Physostigmine (PHY) and galanthamine (GAL) have been identified as two AChEIs with promise as potential treatments for Alzheimer's disease. However, a high degree of variation in patient response to AChEIs has been consistently observed (Kaduszkiewicz et al. 2005). Positron emission tomography (PET) imaging dynamically observes and quantifies receptor availability *in vivo*, which could assess individual response to AChEIs with an appropriate radioligand.

The α4β2 nicotinic acetylcholine receptor (nAChR) has been identified as a target for gauging ACh competition induced by AChEIs with PET. Previous imaging studies have been performed with the PET radioligand 2-[^{18}F]FA-85380 (2-[^{18}F]FA), and a SPECT radioligand 5-[^{123}I]IA-85380 (5-[^{123}I]IA), to inspect for deviations in α4β2 nAChR binding in the presence of AChEIs. Significant reductions in α4β2 availability were found following the administration of PHY in nonhuman primates with 2-[^{18}F]FA (Valette et al. 2005) and 5-[^{123}I]IA (Fujita et al. 2003), and experiments utilizing 5-[^{123}I]IA in humans yielded similar results (Esterlis et al. 2013). No significant changes in distribution volumes were found following GAL administration in nonhuman primates with 2-[^{18}F]FA (Valette et al. 2005). The slow kinetic properties of the radiolabeled 85380 compounds require extended scanning procedures and potentially impair the sensitivity of experiments to detect AChEI-induced effects. A radioligand with faster kinetic properties may dramatically reduce the required scanning time and improve detection of AChEI effects with PET.

The radioligand [^{18}F]nifene is an analog of 2-[^{18}F]FA with similar binding levels and much faster kinetic properties (Hillmer et al. 2012). The rapid kinetics of [^{18}F]nifene present potential improvements for more reliable detection of increased ACh concentrations in addition to shortened scanning procedures. The goal of the present work is to perform a preliminary assessment of [^{18}F]nifene PET sensitivity to competition with synaptic ACh increases induced by both PHY and GAL. Bolus-infusion [^{18}F]nifene experiments were conducted in rats with AChEI administration midway through the scan. Analysis was performed with the linearized parametric neurotransmitter PET model (Normandin et al. 2012) to test for competition at the α4β2 nAChR site post-drug.

Methods

[^{18}F]Nifene was produced following previously published methods (Hillmer et al. 2012). Total yields were in excess of 350 MBq, and specific activities at scan start were greater than 70 GBq/μmol. The *nitro*- precursor was purchased from ABX (Raderberg, Germany). The AChEI drugs physostigmine (PHY) and galanthamine (GAL) were purchased from Akorn, Inc. (Lake Forest, IL) and Sigma-Aldrich (St. Louis, MO), respectively. Two female Sprague-Dawley rats were obtained from Charles River Laboratories, Inc. (Wilmington, MA). Experimental protocols and housing procedures were approved by the institutional animal care and use committee.

Before PET experiments, anesthesia was induced with 5% isoflurane and then maintained at 2–3% isoflurane during PET procedures. Subjects were situated on a heating pad, and heart rate and respiration rate were observed throughout scanning procedures. The brain was

positioned at the isocenter of a Siemens microPET Inveon scanner for image data acquisition. This scanner has a 12.7 cm field of view with a 1.5 mm in-plane spatial resolution (Constantinescu and Mukherjee 2009). Transmission data were acquired before radioligand administration over 15 min with a ^{57}Co source for scatter and attenuation corrections.

PET experiments employed a bolus-infusion (B/I) protocol (Carson et al. 1997). Emission data was acquired for 60 minutes. A total of 34–68 MBq [^{18}F]nifene (≤0.6 nmol total cold nifene) was diluted to a volume of 1 mL. A 150 μL bolus injection was administered with the start of data acquisition, corresponding to a K_{bol} of 20 min, based on our previous experience with [^{18}F]nifene in rhesus monkeys (Hillmer et al., 2012). For the next 60 min, [^{18}F]nifene was infused at a rate of 450 μL/hr. The remainder of the radiotracer volume accounted for the dead volume of the administration line.

Three separate experiments administering PHY, GAL, or saline were performed, in that order for both subjects, to observe the effects of drug on the dynamic PET signal. Experiments were performed at least one week apart to minimize the effects of residual drug on subsequent experiments. Since equilibrium was targeted to occur 20–25 min postinjection, challenge drug was administered 30 min after scan start. Drug was given in 200–300 μL volumes as a 1 min bolus followed by a 200 μL saline flush. PHY was given at a dosage of 100–200 μg/kg, while 5 mg/kg GAL was administered. As a control experiment, a 250 μL saline injection was given to examine changes in PET signal due to vehicle administration.

PET data were histogrammed into 2 minute bins. Data were reconstructed with filtered backprojection using a 0.5 cm^{-1} ramp filter, including corrections for arc, scatter, attenuation, and scanner normalization. Reconstructed images were denoised with HYPR-LR processing (Christian et al. 2010) using a 4×4×4 voxel kernel. The processed images had a matrix size of 128×128×159 with dimensions of 0.78 mm × 0.78 mm × 0.90 mm. Time activity curves (TACs) were extracted from the thalamus (TH) and cortex (CX), regions of elevated [^{18}F]nifene uptake, and the cerebellum (CB), a region of low [^{18}F]nifene uptake. Sets of spheres were manually drawn on late PET frames for regions of high binding, as illustrated in Figure 1. The same number of spheres and slices were used in region identification to maintain inter-scan consistency. Cerebellar regions were defined on early PET frames representing blood flow and visualized on transmission images to ensure no extracerebral voxels were included. A stereotaxic atlas was visually referenced to aid in region identification (Paxinos and Watson 1998). Total volumes of approximately 20 mm^3, 24 mm^3, and 8 mm^3 were defined for the TH, CX, and CB, respectively.

To test for neurotransmitter response to AChEIs, the graphically based linearized parametric neurotransmitter PET model (lp-ntPET) was employed (Normandin et al. 2012). This model extends the multilinear reference tissue model (MRTM) (Ichise et al. 2003) by introducing an activation term with the coefficient γ to modify how the model accounts for specifically bound radioligand. ACh increase was described with a gamma variate function. The time of activation t_D was fixed at 30 min since this parameter was known *a priori* based on the experiment design. A family of gamma variate functions with peak sharpness α and peak time t_P ranging from {0.1, 10} and {31, 120}, respectively, were generated. The lp-ntPET method selected the eigenfunction with the best model fit to the data.

The complete time course of TH and CX PET data were analyzed first with MRTM, then lp-ntPET, using the CB as a reference region. Although specific [^{18}F]nifene cerebellar binding has been previously observed in the rat (Hillmer et al. 2013), the CB served as the most suitable approximation for free radioligand in the absence of blood sampling and alternative

cerebral reference regions. A Bayes-Schwarz Information Criteria (BIC) value, which considers both model fit and the number of model parameters, was calculated for both the lp-ntPET model fit as well as the MRTM model fit. The lower of the BIC values indicates model preference. Preferred lp-ntPET model fits with a negative γ parameter indicated significant competition at the α4β2 nAChR site, while lower BIC values for MRTM indicated no significant PET response to drug.

Results

Relatively constant CB radioligand levels were observed after 20 min, while TH and CX radioligand concentrations took longer to plateau, and in some cases did not achieve constancy before drug administration. The administration of both PHY and GAL elicited visual perturbations to the [^{18}F]nifene TACs, with an apparent faster response from PHY compared to GAL. To ensure stable model fits, a conservative linearization time of 15 min was used, therefore MRTM and lp-ntPET analyses included data from 15 min to scan end. The observed TACs and model fits for the PHY, GAL, and saline studies for subject R2 in the TH are illustrated in Figure 2. In both TH and CX, the BIC value for the lp-ntPET model was preferred in one PHY study and both GAL studies, indicating significant competition at the α4β2 nAChR site during these experiments. During the PHY study with no significant [^{18}F]nifene competition, an obstruction to the radioligand administration line during the experiment confounded interpretation of the PET data. Both sham experiments exhibited no significant ACh activation. ACh response was characterized by a relatively sharp activation curve with $\alpha>4$ for both drugs. The peak time of response was much faster for PHY with $t_P=13$ min postdrug (in TH) as opposed to $t_P\geq30$ min postdrug observed with GAL. The lp-ntPET results are summarized in Table 1 for TH data.

Discussion

The increasing interest in AChEIs as candidate treatments for Alzheimer's disease requires improved examination of the *in vivo* physiological effects of these drugs at the molecular level to compliment the neuropsychological test evaluations used to determine the cognitive outcomes accompanying these drugs. PET imaging holds the potential to fill this need, however, the lack of suitable radioligands has hindered the use of PET in assessing AChEIs. The present studies tested for AChEI perturbations to [^{18}F]nifene TACs using the lp-ntPET model to assess for significant competition at the α4β2 nAChR site by PHY and GAL. The lp-ntPET model was chosen because it does not require blood sampling, flexibly handles single experiment designs including bolus-infusion protocols, and allows for more robust characterization of neurotransmitter surge than its predecessor, LSSRM (Alpert et al., 2003). Three of the four studies with AChEI administration demonstrated statistically significant perturbation of the PET signal using lp-ntPET analysis. To our knowledge, this work contains the first reported sensitivity of a PET radioligand to GAL. Both sham experiments indicated no significant competition, validating that the model was not showing false positive results. A potential weakness is the inability to define an ideal reference region for [^{18}F]nifene in the rat (Hillmer et al. 2013), however, Normandin and colleagues demonstrated with simulations that reference regions with low specific binding may still be suitable if neurotransmitter perturbations are negligible in the non-ideal reference region (2012).

While lp-ntPET can detect neurotransmitter activation and characterize the kinetics of the activation, it does not produce estimates of quantitative changes in binding induced by the drug challenge. Alternative analysis techniques that account for non-equilbrium of radiotracer prior to drug administration and the transient nature of ACh surge induced by AChEIs are required to estimate binding decreases with the present data. Following

previously developed methods (Carson et al., 1997), ratios of radioligand concentrations in the TH and CX relative to CB concentrations (R) measured at the time of peak response (t_P) were preliminarily estimated to decrease by 8% in TH and 9% in CX for 0.1 mg/kg PHY. Dosages of 5 mg/kg GAL elicited estimated decreases in R of 8–10% in TH and 3–5% in CX. Estimates of R in sham experiments yielded values ranging between −4% and 3%, providing insight into the variance of R measurements. These decreases in R must be interpreted as speculative estimates since true equilibrium was not present during these measurements. Blood sampling to acquire an arterial input function would allow for analysis with more advanced modeling techniques, such as parametric-ntPET (Morris et al. 2005). Future studies incorporating complete modeling of the PET data could more accurately quantitate the response of [^{18}F]nifene to AChEIs and assess the validity of candidate reference regions for future lp-ntPET analysis.

The decreases in [^{18}F]nifene levels due to PHY preliminarily estimated herein were lower than previously published values, however, the use of a reference region with specific binding likely underestimated the true value. Reductions in thalamic activities of 14–17% with an analogous PHY dose were observed in rhesus monkeys with 5-[^{123}I]IA (Fujita et al. 2003). Decreases in normalized distribution volumes of 19% and 29% were found in the thalamus and cortex, respectively, when administering an order of magnitude lower PHY dose in humans with 5-[^{123}I]IA (Esterlis et al. 2013). Larger reductions of 20–40% in extrathalamic distribution volumes were observed with a ~450 μg/kg PHY dose given over 3 hours using 2-[^{18}F]FA in baboons (Valette et al. 2005). The work conducted by Esterlis and colleagues administering 1–1.5 mg PHY is the only current study to examine AChEIs in humans at clinically relevant doses, however, their scanning protocols lasted 12 hours due to the slow kinetic properties of the 85380 compounds. Given the dramatically faster kinetic properties of [^{18}F]nifene, future studies using [^{18}F]nifene to examine AChEI sensitivity should be extended to primate species and performed at clinically relevant doses to assess the full potential of imaging AChEI effects with [^{18}F]nifene in patients. The possible effects of anesthesia should also be considered and investigated in future studies.

Previous *in vitro* binding assays found no significant competition of either PHY (<20 μM) or GAL (<4 μM) in the presence of [^{18}F]nifene, suggesting that the drugs themselves did not compete with [^{18}F]nifene at the α4β2 receptor site at the examined levels (Easwaramoorthy et al. 2007). When 100 nM ACh was included with either drug, however, decreases in [^{18}F]nifene levels were observed. These previous findings indicated that bound [^{18}F]nifene was sensitive to ACh competition in the *in vitro* setting. The present work extends these results to provide preliminary observations of AChEIs with [^{18}F]nifene PET in the *in vivo* setting, while the *in vitro* work indicates that the perturbation to [^{18}F]nifene observed herein was likely due to increased ACh concentrations.

The time of peak activation (t_P) determined with the lp-ntPET model was greater for GAL than PHY. This observation can be visualized in the TACs, which showed a faster immediate response to PHY while the GAL response is slower and more subtle (Fig. 2). These findings are in agreement with previous studies, which found GAL to have a slower metabolism rate and prolonged brain presence while being roughly 200 times less potent compared to PHY (Mannens et al. 2002; Jackisch et al. 2009). Since [^{18}F]nifene has an order of magnitude faster tissue clearance rate (k_2) than 2-[^{18}F]FA with similar specific binding and dissociation rates (k_3 and k_4) (Hillmer et al., 2012), it is theoretically more sensitive to competition at the binding site (Morris and Yoder 2007). These differences in kinetic properties may explain the unique sensitivity of [^{18}F]nifene to the slower acting GAL. The peak time of GAL activation was extrapolated to occur after acquisition of PET data was terminated, therefore longer experiments observing t_P should be conducted in the future to completely characterize GAL's effect on ACh fluctuations.

In conclusion, these studies demonstrate the *in vivo* sensitivity of [^{18}F]nifene to PHY and GAL, likely caused by synaptic ACh increases. The short scan times and sensitivity to slower acting drugs with [^{18}F]nifene make it an ideal probe for these competition studies. Future studies should be extended to a primate model and include blood sampling to improve evaluation of [^{18}F]nifene's sensitivity to AChEIs. These initial results are of great importance towards efficiently and accurately evaluating patient response to AChEI drug effects.

Acknowledgments

We thank Professor R. Jerry Nickles, Hector Valdovinos, and Stephen Graves for assistance with radioisotope production, and Elaine Luong for assistance with animal housing. This work was supported by NIH grants MH086014 and T32CA009206.

References

Alpert NM, Badgaiyan RD, Livni E, Fischman AJ. A novel method for noninvasive detection of neuromodulatory changes in specific neurotransmitter systems. Neuroimage. 2003; 19:1049–1060. [PubMed: 12880831]

Bartus RT, Dean RL, Beer B, Lippa AS. The cholinergic hypothesis of geriatric memory dysfunction. Science. 1982; 217:408–417. [PubMed: 7046051]

Carson RE, Breier A, de Bartolomeis A, Saunders RC, Su TP, Schmall B, Der MG, Pickar D, Eckelman WC. Quantification of amphetamine-induced changes in [^{11}C]raclopride binding with continuous infusion. J Cerebr Blood F Met. 1997; 17:437–447.

Christian BT, Vandehey NT, Floberg JM, Mistretta CA. Dynamic PET denoising with HYPR processing. J Nucl Med. 2010; 51:1147–1154. [PubMed: 20554743]

Constantinescu CC, Mukherjee J. Performance evaluation of an Inveon PET preclinical scanner. Phys Med Biol. 2009; 54:2885–2899. [PubMed: 19384008]

Court J, Martin-Ruiz C, Piggott M, Spurden D, Griffiths M, Perry E. Nicotinic receptor abnormalities in Alzheimer's disease. Biol Psychiat. 2001; 49:175–184. [PubMed: 11230868]

Easwaramoorthy B, Pichika R, Collins D, Potkin SG, Leslie FM, Mukherjee J. Effect of acetylcholinesterase inhibitors on the binding of nicotinic α4β2 receptor PET radiotracer, ^{18}F-nifene: A measure of acetylcholine competition. Synapse. 2007; 36:29–36. [PubMed: 17068780]

Esterlis I, Hannestad JO, Bois F, Sewell RA, Tyndale RF, Seibyl JP, Picciotto MR, Laruelle M, Carson RE, Cosgrove KP. Imaging changes in synaptic acetylcholine availability in living human subjects. J Nucl Med. 2013; 54:78–82. [PubMed: 23160789]

Fujita M, Al-Tikriti MS, Tamagnan G, Zoghbi SS, Bozkurt A, Baldwin RM, Innis RB. Influence of acetylcholine levels on the binding of a SPECT nicotinic acetylcholine receptor ligand [^{123}I]5-I-A-85380. Synapse. 2003; 48:116–122. [PubMed: 12645036]

Hillmer AT, Wooten DW, Slesarev MS, Ahlers EO, Barnhart TE, Murali D, Schneider ML, Mukherjee J, Christian BT. PET imaging of α4β2* nicotinic acetylcholine receptors: Quantitative analysis of ^{18}F-nifene kinetics in the nonhuman primate. J Nucl Med. 2012; 53:1471–1480. [PubMed: 22851633]

Hillmer AT, Wooten DW, Farhoud M, Barnhart TE, Mukherjee J, Christian BT. The effects of lobeline on α4β2* nicotinic acetylcholine receptor binding and uptake of [^{18}F]nifene in rats. J Neurosci Methods. 2013; 214:163–169. [PubMed: 23370310]

Hogg RC, Raggenbass M, Bertrand D. Nicotinic acetylcholine receptors: From structure to brain function. Rev Physiol Biochem Pharmacol. 2003; 147:1–46. [PubMed: 12783266]

Ichise M, Liow J-S, Lu J-Q, Takano A, Model K, Toyama H, Suhara T, Suzuki K, Innis RB, Carson RE. Linearized reference tissue parametric imaging methods: application to [^{11}C]DASB positron emission tomography studies of the serotonin transporter in human brain. J Cerebr Blood F Met. 2003; 23:1096–1112.

Jackisch R, Förster S, Kammerer M, Rothmaier AK, Ehret A, Zentner J, Feuerstein TJ. Inhibitory potency of choline esterase inhibitors on acetylcholine release and choline esterase activity in fresh

specimens of human and rat neocortex. J Alzheimers Dis. 2009; 16:635–647. [PubMed: 19276558]

Kaduszkiewicz H, Zimmerman T, Beck-Bornholdt H-P, van den Bussche H. Cholinesterase inhibitors for patients with Alzheimer's disease: Systematic review of randomised clinical trials. BMJ. 2005; 331:321–327. [PubMed: 16081444]

Mannens GSJ, Snel CAW, Hendrickx J, Verhaeghe T, le Jeune L, Bode W, van Beijsterveldt L, Lavrijsen K, Leempoels J, van Osselaer N, van Peer A, Meuldermans W. The metabolism and excretion of galantamine in rats, dogs, and humans. Drug Metab Dispos. 2002; 30:553–563. [PubMed: 11950787]

Morris ED, Yoder KK, Wang C, Normandin MD, Zheng Q-H, Mock B, Muzic RF, Froehlich JC. ntPET: A new application of PET imaging for characterizing the kinetics of endogenous neurotransmitter release. Mol Imaging. 2005; 4:473–489. [PubMed: 16285909]

Morris ED, Yoder KK. Positron emission tomography displacement sensitivity: Predicting binding potential change for positron emission tomography tracers based on their kinetic characteristics. J Cerebr Blood F Met. 2007; 27:606–617.

Normandin MD, Schiffer WK, Morris ED. A linear model for estimation of neurotransmitter response profiles from dynamic PET data. NeuroImage. 2012; 59:2689–2699. [PubMed: 21767654]

Paxinos, G.; Watson, C. The Rat Brain in Sterotaxic Coordinates. 4th ed.. San Diego: Academic Press; 1998.

Valette H, Bottlaender M, Dolle R, Coulon C, Ottaviani M, Syrota A. Acute effects of physostigmine and galantamine on the binding of [^{18}F]Fluoro-A-85380: A PET study in monkeys. Synapse. 2005; 56:217–221. [PubMed: 15803498]

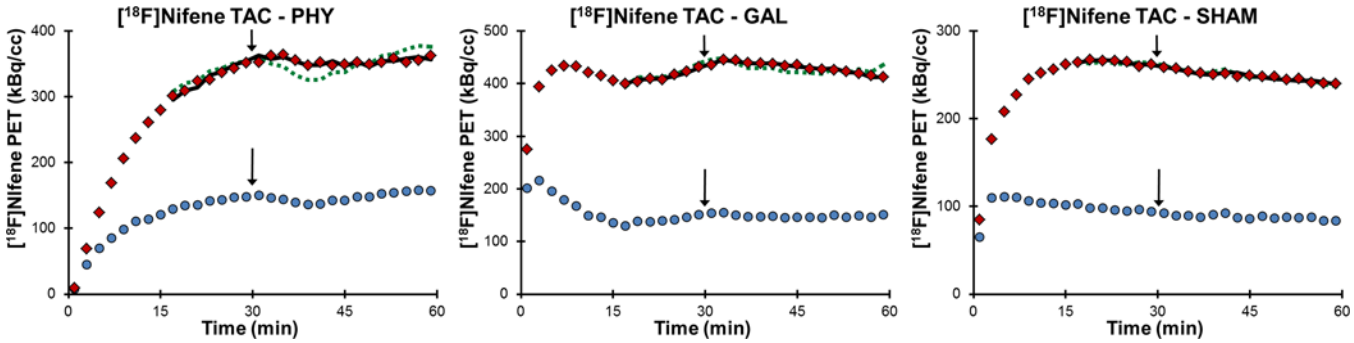

Figure 1.

Region of interest definition for the thalamus (TH), cortex (CX), and cerebellum (CB) in the rat. The images are late summed PET frames of [^{18}F]nifene uptake. The solid lines in the sagittal plane indicate the location of the corresponding coronal and transverse slices, while dotted line in the transverse plane indicates the location of the sagittal plane.

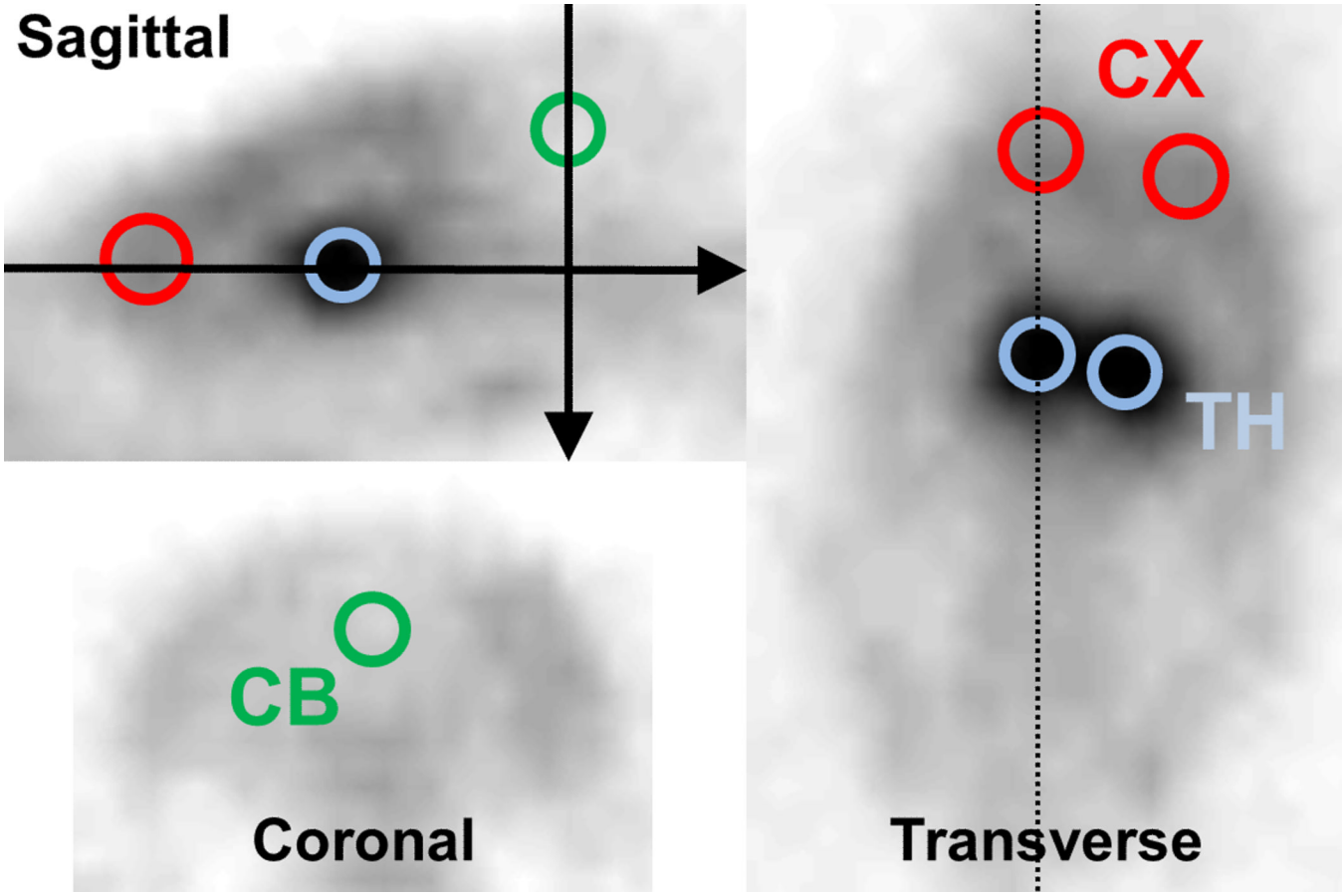

Figure 2.

[^{18}F]Nifene PET time-activity curves for subject R2, with administration of physostigmine (left), galanthamine (center), and saline (right). Time of drug administration at 30 min is denoted by the arrows. Regions shown include the thalamus (diamonds) and cerebellum (circles). Model fits with MRTM (dashed line) and lp-ntPET (solid line) are included for the thalamus data with the cerebellum as a reference region. Significant acetylcholine activation was detected in both drug experiments but not the sham experiment as evidenced by the improved fit with the lp-ntPET model and the observed bias with MRTM.

Table 1

Experiment Design and Results

Subject	Drug	Dosage	MRTM BIC Value	lp-ntPET BIC Value	Significant Activation?	$\alpha^{\dagger}$	$t_p{}^{\dagger}$
R1	PHY	0.2 mg/kg	51.9*	52.7	NO	-	-
R2	PHY	0.1 mg/kg	67.0	51.8*	YES	4	43
R1	GAL	5 mg/kg	59.8	36.7*	YES	10	60
R2	GAL	5 mg/kg	50.9	46.8*	YES	4	90
R1	SHAM	N/A	31.6*	42.1	NO	-	-
R2	SHAM	N/A	N/A^	N/A^	NO	-	-

*Denotes the lower (preferred) of the two MRTM (null condition) and lp-ntPET (ACh activation) BIC values.

^A positive value of γ (e.g. decrease in neurotransmitter competition) was determined for this study with lp-ntPET.

†These values were based on the results of the lp-ntPET model. No values were included if significant activation was not measured.